tion, our data imply a direct role of the gene for a transcription factor in human cancer-associated genetic rearrangements. Although it is suspected that Myc may also function as a transcription factor, direct demonstration of this has not been presented. Finally, given our data suggesting that a potential fusion transcript may be formed as a result of t(1;19), it should be possible to design DNA probe–based methodologies to detect this abnormality in leukemia DNAs. Knowledge of the genes affected by the t(1;19) should also help establish whether submicroscopic lesions of *E2A* or a gene on chromosome 1 are associated with various leukemias that lack the t(1;19) chromosomal translocation.

Note added in proof: Recent review of the karyotype for leukemia cells from patient 1 showed that although this leukemia carries a chromosome 19 abnormality, it is not a t(1;19) or its unbalanced variant (*24*). Therefore, ten out of ten t(1;19) breakpoints in this study were detected by using the pE47M probe, suggesting that all t(1;19) breakpoints occur near or within *E2A*.

REFERENCES AND NOTES

1. F. Mitelman, *Catalog of Chromosome Aberrations in Cancer* (Liss, New York, 1988); S. Heim and F. Mitelman, *Cancer Cytogenetics* (Liss, New York, 1987).
2. A. J. Carroll *et al.*, *Blood* **63**, 721 (1984); P. M. Michael, M. D. Levin, O. M. Garson, *Cancer Genet. Cytogenet.* **12**, 333 (1984); D. L. Williams *et al.*, *Cell* **36**, 101 (1984); P. M. Michael, O. M. Garson, D. F. Callen, *Cancer Genet. Cytogenet.* **17**, 79 (1985).
3. T. L. Yang-Feng, U. Francke, A. Ullrich, *Science* **228**, 728 (1985); R. S. K. Chaaganti *et al.*, *Cytogenet. Cell Genet.* **43**, 181 (1986).
4. A. K. Hatzopoulos, U. Schlokat, P. Gruss, in *Eukaryotic RNA Synthesis and Processing*, B. D. Hames and D. M. Glover, Eds. (Horizons in Molecular Biology Series, IRL Press, Oxford, 1988), pp. 43–96.
5. G. M. Church, A. Ephrussi, W. Gilbert, S. Tonegawa, *Nature* **313**, 798 (1985); A. Ephrussi, G. M. Church, S. Tonegawa, W. Gilbert, *Science* **227**, 134 (1985); J. Weinberger, D. Baltimore, P. A. Sharp, *Nature* **322**, 846 (1986).
6. R. Sen and D. Baltimore, *Cell* **46**, 705 (1986).
7. M. Lenardo, J. W. Pierce, D. Baltimore, *Science* **236**, 1573 (1987).
8. C. Murre, P. S. McCaw, D. Baltimore, *Cell* **56**, 777 (1989).
9. X. H. Sun and D. Baltimore, unpublished observations.
10. R. L. Davis, H. Weintraub, A. B. Lassar, *Cell* **51**, 987 (1987); M. C. Alonso and C. V. Cabrera, *EMBO J.* **7**, 2585 (1988); M. Caudy *et al.*, *Cell* **55**, 1061 (1988); E. Legouy *et al.*, *EMBO J.* **6**, 3359 (1987); L. W. Stanton, M. Schwab, J. M. Bishop, *Proc. Natl. Acad. Sci. U.S.A.* **83**, 1772 (1986); B. Thisse, C. Stoetzel, C. Gorostiza-Thisse, F. Perrin-Schmitt, *EMBO J.* **7**, 2175 (1988); R. Villares and C. V. Cabrera, *Cell* **50**, 415 (1987); W. E. Wright, D. A. Sassoon, V. K. Lin, *ibid.* **56**, 607 (1989).
11. J. D. Mellentin, S. D. Smith, M. L. Cleary, *Cell* **58**, 77 (1989).
12. F. W. Alt *et al.*, *Cold Spring Harbor Symp. Quant. Biol.* **51**, 931 (1986).
13. For in situ hybridizations, pE47M was labeled to a specific activity of 7.9×10^8 cpm/μg by hexamer priming [A. P. Feinberg and B. Vogelstein, *Anal. Biochem.* **132**, 6 (1984)]. Hybridization to chromosome preparations from a chromosomally normal female was carried out at 44°C at a final probe concentration of 10 pg/μl [M. E. Harper and G. F. Saunders, *Chromosoma* **83**, 431 (1981)]. The preparations were exposed for 5 days, and then developed and analyzed [T. A. Donlon, M. Litt, S. R. Newcom, R. E. Magenis, *Am. J. Hum. Genet.* **35**, 1097 (1984)]. Additional studies, in which less stringent hybridization conditions were used, showed a primary hybridization peak at chromosome bands 19p13.2–p13.3 and a possible secondary site on chromosome 9p (T. A. Donlon, unpublished data).
14. J. D. Brook, D. J. Shaw, L. Meredith, G. A. Brun, P. S. Harper, *Hum. Genet.* **68**, 282 (1984); A. J. Lusis *et al.*, *Proc. Natl. Acad. Sci. U.S.A.* **83**, 3929 (1986).
15. J. D. Mellentin, J. Nourse, M. L. Cleary, unpublished observations.
16. H. W. Findley *et al.*, *Blood* **60**, 1305 (1982); R. J. Green, H. W. Findley, Jr., A. T. L. Chen, A. H. Ragab, *Cancer Genet. Cytogenet.* **7**, 257 (1982). The cell line 697 was originally described as having a t(7;19)(q11;q13) chromosomal translocation, but subsequent review showed that it carries an unbalanced t(1;19)(q13;p13) [P. E. Barker, A. J. Carroll, M. D. Cooper, *ibid.* **25**, 379 (1987); A. J. Carroll, unpublished observations].
17. Cell line SUP-B27 was established from an individual with pre-B cell ALL under conditions similar to those previously described (*18*). Karyotype studies showed that the cell line was representative of the patient's leukemia because both carried a reciprocal t(1;19) and trisomy chromosome 8 as the only detectable cytogenetic abnormalities (S. D. Smith, T. A. Donlon, M. L. Cleary, unpublished data).
18. S. D. Smith *et al.*, *Blood* **71**, 395 (1988); S. D. Smith *et al.*, *ibid.*, in press.
19. J. D. Mellentin and M. L. Cleary, unpublished observations.
20. N. Galili and M. L. Cleary, unpublished observations.
21. C. Murre and D. Baltimore, unpublished observations.
22. M. L. Cleary *et al.*, *Cell* **47**, 19 (1986).
23. A. Epstein *et al.*, *Cancer* **42**, 2379 (1978); S. H. Doi *et al.*, *Blood* **70**, 1619 (1987).
24. A. G. Carroll, unpublished observations.

25. We thank the late S. A. Latt for initial indications that *E2A* might map to chromosome 19, P. Verzola for photography, G. Bruns and T. Mohandas for somatic cell hybrid DNAs, and W. Crist and the Pediatric Oncology Group, St. Louis, MO, for providing leukemia cells carrying the t(1;19). Supported by grants from NIH (CA42971, CA30969, CA42106, CA33603, CA31566, and GM39458) and a grant from the Lucille P. Markey Charitable Trust. J.D.M. was supported in part by PHS grant NRSA 5T32 CA09302. C.M. is supported by a grant from the Leukemia Society of America. D.B. is supported by a grant from the American Cancer Society. M.L.C. is a scholar of the Lucille P. Markey Charitable Trust.

13 June 1989; accepted 28 August 1989

A Role for a 70-Kilodaton Heat Shock Protein in Lysosomal Degradation of Intracellular Proteins

HUI-LING CHIANG,* STANLEY R. TERLECKY, CHARLES P. PLANT, J. FRED DICE†

A 73-kilodalton (kD) intracellular protein was found to bind to peptide regions that target intracellular proteins for lysosomal degradation in response to serum withdrawal. This protein cross-reacted with a monoclonal antibody raised to a member of the 70-kD heat shock protein (hsp70) family, and sequences of two internal peptides of the 73-kD protein confirm that it is a member of this family. In response to serum withdrawal, the intracellular concentration of the 73-kD protein increased severalfold. In the presence of adenosine 5′-triphosphate (ATP) and $MgCl_2$, the 73-kD protein enhanced protein degradation in two different cell-free assays for lysosomal proteolysis.

STUDIES OF THE DEGRADATION OF proteins microinjected into cultured cells have shown that ribonuclease A (RNase A) is degraded within lysosomes and that lysosomal degradation of RNase A is increased when cells are deprived of serum growth factors. The increased degradation during serum withdrawal results from an increased rate of protein transfer to lysosomes (*1, 2*).

Amino acid residues 7 to 11 (KFERQ) (*3*) of RNase A constitute the essential region for the enhanced degradation (*4*), and similar, but not identical, peptide sequences exist in fibroblast proteins that are preferentially degraded when cells are deprived of serum (*5*). A detailed description of the probable peptide motif has been presented (*6*).

To determine whether cytosolic proteins participate in the lysosomal proteolysis of microinjected RNase A seen in response to serum withdrawal, we looked for proteins that could specifically recognize KFERQ. We found a 73-kD protein in the cytosol of serum-deprived fibroblasts that bound to RNase S-peptide (residues 1 to 20 of RNase A) linked to Sepharose (but not to underivatized Sepharose) and could be eluted with the peptide KFERQ (Fig. 1), RNase S-peptide, or RNase A, but not by several unrelated peptides or proteins (7). We refer to this protein as the 73-kD peptide recognition protein (prp73). A smaller protein (30

Department of Physiology, Tufts University School of Medicine, Boston, MA 02111.

*Present address: Department of Biochemistry, University of California, Berkeley, CA 94720.
†To whom correspondence should be addressed.

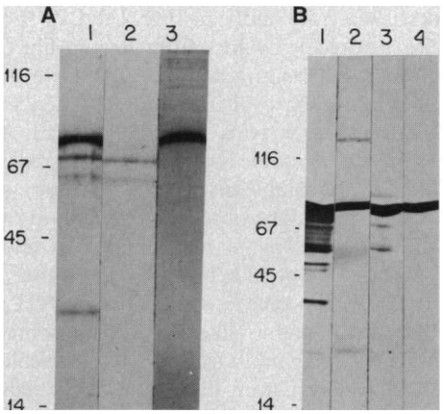

Fig. 1. A 73-kD cellular protein binds to RNase S-peptide and is recognized by MAb 7.10. (**A**) IMR-90 human diploid lung fibroblasts were grown as described (*2*). Cytosolic proteins from serum-deprived fibroblasts and from livers of fed rats were prepared (*5*) and passed through a 10-ml column of RNase S-peptide–Sepharose. The column was washed with 20 column-volumes of 0.5*M* tris buffer (*p*H 8) containing 0.5*M* NaCl and then with 5 column-volumes of phosphate-buffered saline (*p*H 7.2) containing 0.5*M* NaCl and 0.1% Triton X-100. Proteins that remained associated with the RNase S-peptide–Sepharose were eluted by excess KFERQ peptide (2.5 mg/ml). Eluted proteins were visualized after SDS–polyacrylamide gel electrophoresis (SDS-PAGE) with silver stain (lane 1) or Coomassie blue R-250 (lane 3). Lane 2 contained sample buffer with no protein added and was silver-stained; this shows that the two faint bands with molecular sizes of 60 to 70 kD are artifacts (*26*). Protein standards (Sigma) were as follows: 116 kD, *E. coli* β-galactosidase; 67 kD, bovine serum albumin; 45 kD, ovalbumin; and 14 kD, lysozyme. (**B**) Protein blots with MAb 7.10. Lane 1, purified hscp73 from bovine brain; lane 2, whole cytosol from rat liver; lane 3, purified prp73 from rat liver; and lane 4, purified prp73 from human fibroblasts. Immunoblotting was performed according to the manufacturer's instructions (Bio-Rad), except bovine serum albumin, rather than gelatin, was used in the blocking solution and antibody buffer. MAb 7.10 was in the form of a hybridoma culture medium and was used at a 1:50 dilution. The MAb 7.10 was visualized with biotinylated goat antibody to rat immunoglobin G (Sigma) and a mixture of biotinylated horseradish peroxidase and avidin.

Table 1. Amino acid sequences of prp73 and other hsp70 proteins. Purified prp73 from rat liver was subjected to SDS–PAGE and stained with Coomassie blue. Fragment 1 was generated with staphylococcal V8 protease (Sigma). Fragment 2 was a product of spontaneous hydrolysis of prp73. After electrophoresis, the fragments of prp73 were transferred onto Immobilon (Millipore) and visualized by brief staining with Coomassie blue. Bands were cut out and sequenced with a pulsed-liquid protein sequencer (Applied Biosystems Model 477A) and an on-line phenylthiohydantoin amino acid analyzer (Applied Biosystems Model 120A). Differences between prp73 and the corresponding sequences of other hsp70's are underlined. Sequences were obtained from published reports (*25*). X, unknown residue (*3*).

Protein	Fragment 1	Fragment 2	Identity (%)
Rat prp73	V K S T A G D T X L	G D A A K X X V A	
Rat hscp73	V K S T A G D T H L	G D A A K N Q V A	100
Human hsp70	V K A T A G D T H L	G D A A K N Q A A	88
Chicken hsp70	V K S T A G D T H L	G D A A K N Q V A	100
Trout hsp70	V K A T A G D T H L	G D A A K N Q V A	94
Frog hsp70	V K A T A G D T H L	G D A A K N Q V A	94
Drosophila hsp70	V R S T A G D T H L	G E P A K N Q V A	81
Yeast ssa1	V K A T A G D T H L	G D A A K N Q A A	88
Yeast ssa2	V K S T A G N T H L	G D A A K N Q A A	88
E. coli *dnaK* product	V L A T N G N T H L	G Q P A K R Q A V	50
Rat grp78	V V A T N G D T H L	G D A A K N Q L T	69
Chicken grp78	V V A T N G D T H L	G D A A K N Q L T	69

kD) was evident in some silver-stained preparations (Fig. 1) and is probably a breakdown product of prp73 (*8*).

Protein blot analysis showed that a rat monoclonal antibody (MAb 7.10) to *Drosophila* hsp70, which recognizes all known hsp70's from organisms as diverse as yeast and humans (*9, 10*), also recognized (i) the 73-kD heat shock cognate protein (hscp73) from bovine brain (*11*) and some of its degradative products (*8*), (ii) a major 73-kD protein, as well as some minor proteins, in rat liver cytosol, and (iii) purified prp73 from both rat liver and human fibroblasts (Fig. 1).

Eukaryotic organisms contain eight to ten different proteins of the hsp70 family (*9, 12*). Some of these proteins are not induced by heat, but by other stimuli such as cold exposure (*13*), glucose deprivation (*10, 14*), or growth factor stimulation (*10*). Proposed roles for different hsp70's include facilitation of ribosome assembly (*15*), cytoskeletal rearrangement (*16*), uncoating of clathrin-coated vesicles (*17*), and retarding movement through the endoplasmic reticulum of incompletely assembled multimeric proteins and underglycosylated or denatured proteins (*14*). Also, hsp70's in yeast facilitate protein import into mitochondria and microsomes (*18, 19*).

Amino acid sequence analysis confirmed that prp73 is a member of the hsp70 family. The determined amino acid sequence of fragments of prp73 isolated from rat liver show 100% identity with rat hscp73 and chicken hsp70 (Table 1). The sequences also share 50 to 94% identity with other members of the hsp70 family.

We examined the effects of serum withdrawal on the amount and subcellular distribution of hsp70's by protein blotting with MAb 7.10. Most hsp70's fractionated with organelles in cells that had been maintained in the presence of serum; in response to serum withdrawal, the concentration of hsp70's increased in all cell fractions, but

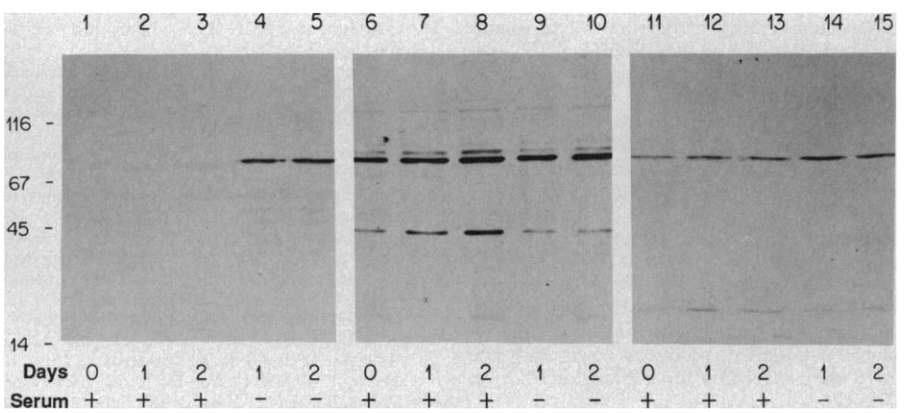

Fig. 2. Increase in the amount of cytosolic prp73 in response to serum withdrawal. Confluent cultures of fibroblasts were maintained in the presence or absence of 10% fetal bovine serum for 0, 1, or 2 days, harvested, and subjected to subcellular fractionation as described (*5*). Equal amounts of protein (100 μg) from cytosol (lanes 1 to 5), a fraction containing mitochondria and lysosomes (lanes 6 to 10), and a fraction containing microsomes and ribosomes (lanes 11 to 15) were separated by SDS-PAGE. The proportion of cell protein in the cytosol, mitochondria-lysosomes, and microsomes-ribosomes is 57%, 6%, and 4%, respectively (*5*). Protein standards and immunoblotting procedures were as described (Fig. 1). Immunoblots were quantitated with a Bio-Rad 620 Video Densitometer in the reflectance mode.

most strikingly in cytosol (Fig. 2). The predominant hsp70 in the cytosol of serum-deprived human fibroblasts appears to be prp73 because most (>90%) of the immunoreactive protein could be removed by affinity chromatography over an RNase S-peptide–Sepharose column, and other hsp70's do not bind to such columns (*20*). Quantitation of the protein blots indicated that there was a 20-fold induction of prp73 in cytosol, a 1.4-fold induction in a fraction containing mitochondria and lysosomes, and a 1.9-fold induction in a fraction containing microsomes and ribosomes in cells that had been deprived of serum for 1 day. We cannot rule out the possibility that the modest increase in prp73 in organelle fractions after serum withdrawal was due to a trace amount of contaminating cytosol.

To obtain more direct evidence for a role of prp73 in the lysosomal uptake and degradation of RNase A, we attempted to reconstitute this degradative pathway in two different cell-free systems. Digitonin-permeabilized Chinese hamster ovary (CHO) cells show increased rates of lysosomal proteolysis if cells are deprived of serum before they are permeabilized (*21*). We microinjected labeled RNase A into CHO cells and found that it was degraded at a similar rate to that seen in human fibroblasts; its half-life was 90 hours in the presence of serum and 40 hours in the absence of serum (*22*). We permeabilized CHO cells with digitonin as described [(*21*) and legend to Table 2] and also isolated lysosomes from human fibroblasts by consecutive density gradients [(*23*) and the legend to Table 2]. We added to both cell-free systems ^{3}H-labeled RNase A or RNase S-peptide and measured degradation to acid-soluble material under a variety of conditions. The observed degradation of [^{3}H]RNase A by permeabilized cells and [^{3}H]RNase S-peptide by isolated lysosomes required adenosine 5′-triphosphate (ATP) and $MgCl_2$ and is likely to be lysosomal because it was inhibited by NH_4Cl (Table 2). The degradation in isolated lysosomes was also temperature-dependent and saturable, and addition of prp73 significantly stimulated degradation of RNase A and RNase S-peptide in both cell-free systems (Table 2). Two other hsp70's, the glucose-regulated 78-kD protein (grp78) and the *Escherichia coli dnaK* product, had no effect (*24*). The maximal degradation rates achieved were 0.44% per hour for permeabilized cells and 2.1% per hour for isolated lysosomes. These rates correspond to half-lives of 157 hours and 33 hours, respectively, reasonably close to half-lives observed for RNase A microinjected into intact cells.

Our working model for the role that prp73 plays in the lysosomal degradation of cytosolic proteins containing KFERQ-like sequences is as follows: when cells are deprived of serum, the amount of prp73 increases and the protein appears in the cytosol where the proteins to be degraded reside; prp73 recognizes the KFERQ-like sequences within proteins that are destined for lysosomal degradation and then alters the conformation of these proteins into a transport competent state, analogous to the proposed role of hsp70's in the translocation of proteins into microsomes and mitochondria (*18, 19*). The organelle specificity for the protein translocation may reside with the particular hsp70 involved, organelle receptors for the hsp70-protein complex, or both.

Table 2. Stimulation of degradation of [^{3}H]RNase A and [^{3}H]RNase S-peptide by prp73 in permeabilized cells and by isolated lysosomes. CHO cells were scraped from the monolayer in cytoskeletal buffer (*21*), centrifuged at 800g for 5 min, and permeabilized with digitonin essentially as described (*21*). The resulting permeabilized cells lost >90% of cytosolic enzymes and retained >90% of organelle enzymes. The degradation mixture contained 6×10^6 permeabilized cells, 100,000 dpm of [^{3}H]RNase A (5×10^6 dpm/μg), and 5 μg of cytosolic proteins in a final volume of 0.5 ml. Other factors added were at the following final concentrations: ATP and an ATP-regenerating system [10 m*M* ATP, 10 m*M* $MgCl_2$, 2 m*M* phosphocreatine, and creatine phosphokinase (50 μg/ml)], NH_4Cl (10 m*M*), and prp73 (10 μg/ml). Degradation was linear for 2 hours at 25°C, and after 2 hours phosphotungstate-HCl–soluble radioactivity was determined (*2*). Acid-soluble radioactivity in the absence of permeabilized cells (14 dpm) has been subtracted from the data ($n = 6$). Similar results were obtained in two other experiments. Lysosomes were isolated from serum-supplemented human IMR-90 fibroblasts by two consecutive discontinuous density gradient centrifugations as described (*23*). Lysosomes from 2×10^6 cells were incubated with 10,000 dpm of [^{3}H]RNase S-peptide (5×10^6 dpm/μg). Other additions and reagents were as described for CHO cells except that unlabeled RNase S-peptide and the peptide KFERQ were added to a final concentration of 500 μg/ml and 4.0 μg/ml, respectively ($n = 4$). Similar results were obtained in five other experiments. Control experiments showed linear degradation for 2 hours at 25°C, equivalent percent degradation within a tenfold range of labeled substrate added, and no degradation without added lysosomes. In experiment 2, the acid-soluble radioactivity produced when ATP and prp73 were incubated for 2 hours at 0°C was 47 ± 17.

Assay system	Additions	Acid-soluble radioactivity (dpm) (mean ± SD)
Permeabilized CHO cells and [^{3}H]RNase A	None	1 ± 8
	ATP	250 ± 17
	ATP + NH_4Cl	22 ± 6
	ATP + prp73	876 ± 154
	Experiment 1	
Isolated lysosomes and [^{3}H]RNase A S-peptide	None	73 ± 5
	ATP	152 ± 6
	ATP + prp73	214 ± 4
	ATP + prp73 + S-peptide	22 ± 2
	Experiment 2	
	ATP + prp73	425 ± 46
	ATP + prp73 + NH_4Cl	11 ± 30
	ATP + prp73 + KFERQ	326 ± 32

REFERENCES AND NOTES

1. J. F. Dice, *FASEB J.* **1**, 349 (1987); M. A. McElligott, P. Miao, J. F. Dice, *J. Biol. Chem.* **260**, 11986 (1985); N. T. Neff, L. Bourret, P. Miao, J. F. Dice, *J. Cell Biol.* **91**, 184 (1981); R. Gurley and J. F. Dice, *Cell Biol. Int. Rep.* **12**, 885 (1988).
2. J. M. Backer, L. Bourret, J. F. Dice, *Proc. Natl. Acad. Sci. U.S.A.* **80**, 2166 (1983).
3. Abbreviations for the amino acid residues are A, Ala; C, Cys; D, Asp; E, Glu; F, Phe; G, Gly; H, His; I, Ile; K, Lys; L, Leu; M, Met; N, Asn; P, Pro; Q, Gln; R, Arg; S, Ser; T, Thr; V, Val; W, Trp; and Y, Tyr.
4. J. F. Dice, H.-L. Chiang, E. P. Spencer, J. M. Backer, *J. Biol. Chem.* **261**, 6853 (1986).
5. H.-L. Chiang and J. F. Dice, *ibid.* **263**, 6797 (1988).
6. J. F. Dice and H.-L. Chiang, *Biochem. Soc. Symp.* **55**, 45 (1989).
7. H.-L. Chiang and J. F. Dice, unpublished observations.
8. H. K. Mitchell and N. S. Petersen, *J. Biol. Chem.* **262**, 14298 (1987); preparations of prp73 and hscp73 that are initially single bands at 73 kD subsequently appear as proteins of 45 kD, 30 kD, and 14 kD.
9. S. Lindquist, *Annu. Rev. Biochem.* **55**, 1151 (1986); ——— and E. A. Craig, *Annu. Rev. Genet.* **22**, 631 (1988).
10. S. S. Watowich and R. I. Morimoto, *Mol. Cell Biol.* **8**, 393 (1988).
11. P. T. J. Guidon and L. E. Hightower, *J. Cell Physiol.* **128**, 239 (1986).
12. D. G. Lowe and L. A. Moran, *Proc. Natl. Acad. Sci. U.S.A.* **81**, 2317 (1984); K. L. Milarski and R. I. Morimoto, *ibid.* **83**, 9517 (1986); M. Werner-Washburne *et al.*, *Mol. Cell Biol.* **7**, 2568 (1987); M. L. Pardue, J. Feramisco, S. Lindquist, Eds., *Stress-Induced Proteins* (Liss, New York, 1989).
13. M. S. Ellwood and E. A. Craig, *Mol. Cell Biol.* **4**, 1454 (1984).
14. S. Munro and H. R. B. Pelham, *Cell* **46**, 291 (1986).
15. W. J. Welch and J. R. Feramisco, *J. Biol. Chem.* **259**, 1493 (1984).
16. E. W. Napolitano *et al.*, *ibid.* **262**, 1493 (1987).
17. T. G. Chappell *et al.*, *Cell* **45**, 3 (1986).
18. R. J. Deshaies *et al.*, *Nature* **332**, 800 (1988).
19. W. Chirico, M. G. Waters, G. Blobel, *ibid.*, p. 805.
20. S. R. Terlecky and J. F. Dice, unpublished observations.
21. D. Leonard and H. Chen, *Biochim. Biophys. Acta* **968**, 269 (1988).
22. L. Jeffreys and J. F. Dice, unpublished observations.
23. E. A. Madden, J. B. Wirt, B. Storrie, *Arch. Biochem. Biophys.* **257**, 27 (1987).
24. L. Jeffreys, S. R. Terlecky, J. F. Dice, unpublished observations.
25. References for published sequences are as follows: Rat hscp73: K. O'Malley, A. Mauron, J. D. Barchas, L. Kedes, *Mol. Cell Biol.* **5**, 3476 (1985); human hsp70: C. Hunt and R. I. Morimoto, *Proc. Natl. Acad. Sci. U.S.A.* **82**, 6455 (1985); chicken hsp70: R. I. Morimoto *et al.*, *J. Biol. Chem.* **261**, 12692 (1986); trout hsp70: R. K. Kothary *et al.*, *Mol. Cell Biol.* **4**, 1785 (1984); frog hsp70: M. Bienz, *Proc. Natl. Acad. Sci. U.S.A.* **81**, 3138 (1984); *Drosophila*

hsp70: T. D. Ignolia, E. A. Craig, B. J. McCarthy, *Cell* **21**, 669 (1980); yeast ssa1 and ssa2 (formerly called YG100 and YG101): T. D. Ignolia, M. R. Slater, E. A. Craig, *Mol. Cell Biol.* **2**, 1388 (1982); *E. coli dnaK* product: J. Bardwell and E. A. Craig, *Proc. Natl. Acad. Sci. U.S.A.* **81**, 848 (1984); rat grp78: S. Munro and H. R. B. Pelham, *Cell* **46**, 291 (1986); and chicken grp78: M. Y. Stoeckle *et al.*, *Mol. Cell Biol.* **8**, 2675 (1988).
26. T. Marshall and K. M. Williams, *Anal. Biochem.* **139**, 502 (1984).
27. We thank S. Sadis and L. Hightower for helpful discussions and for providing purified bovine hscp73, bovine grp78, and *E. coli dnaK* product; S. Lindquist and L. Hightower for the MAb 7.10; M. Berne for the peptide sequencing; and J. Faust, M. Forgac, G. Sahagian, and I. Arias for critical review of the manuscript. Supported by NIH grants AG06116 and DK07542.

5 June 1989; accepted 29 August 1989

The Neostriatal Mosaic: Striatal Patch-Matrix Organization Is Related to Cortical Lamination

CHARLES R. GERFEN

The basal ganglia, of which the striatum is the major component, process inputs from virtually all cerebral cortical areas to affect motor, emotional, and cognitive behaviors. Insights into how these seemingly disparate functions may be integrated have emerged from studies that have demonstrated that the mammalian striatum is composed of two compartments arranged as a mosaic, the patches and the matrix, which differ in their neurochemical and neuroanatomical properties. In this study, projections from prefrontal, cingulate, and motor cortical areas to the striatal compartments were examined with the *Phaseolus vulgaris*–leucoagglutinin (PHA-L) anterograde axonal tracer in rats. Each cortical area projects to both the patches and the matrix of the striatum; however, deep layer V and layer VI corticostriatal neurons project principally to the patches, whereas superficial layer V and layer III and II corticostriatal neurons project principally to the matrix. The relative contribution of patch and matrix corticostriatal projections varies among the cortical areas examined such that allocortical areas provide a greater number of inputs to the patches than to the matrix, whereas the reverse obtains for neocortical areas. These results demonstrate that the compartmental organization of corticostriatal inputs is related to their laminar origin and secondarily to the cytoarchitectonic area of origin.

THE STRIATUM, WHICH COMPRISES the caudate, putamen, and accumbens nuclei, is composed of two distinct compartments, termed the patches and matrix, that are arranged as a mosaic (*1–4*). Neurochemical markers are differentially distributed in these compartments. For example, patches are rich in μ-opiate receptor binding sites (*3*), whereas the matrix contains calbindin D_{28kD} immunoreactive neurons and a rich plexus of somatostatin fibers (*5*). Neuroanatomical studies have established that the compartmental patterns of cortical (*2, 4, 6, 7*), thalamic (*3, 8*), and dopaminergic (*9*) inputs and the patterns of the outputs of the patches and matrix (*4, 5, 10*) reflect segregated input-output systems. Previous studies have related the compartmental organization of corticostriatal inputs to the cortical area of origin (*4, 6*), that is, the prelimbic cortex has been shown to project to the patch compartment, whereas most neocortical areas examined, including motor and visual cortices, have been shown to project to the matrix. The prelimbic cortex receives major inputs from limbic brain areas, including the amygdala (*11*), and the amygdala has been shown to project directly to the patches (*12*). These findings might suggest that limbic-related systems provide the major input to the patches, whereas neocortical areas provide inputs to the matrix. Before accepting as a general rule this allocortical versus neocortical segregation of patch and matrix inputs, a more thorough examination of the compartmental organization of corticostriatal projections was initiated.

Iontophoretic injections of the anterogradely transported axonal tracer *Phaseolus vulgaris*–leucoagglutinin (PHA-L) (*13*) were stereotaxically placed into the frontal cortex of 150 adult Sprague-Dawley rats. After 2 weeks the brains were processed by standard immunohistochemical procedures (*14*) to localize the PHA-L, which had been incorporated into neurons at the injection site in the cortex and anterogradely transported in the axons. Adjacent sections through the striatum were processed for immunohistochemical staining of calbindin D_{28kD}, a striatal matrix-specific marker (*5*), to identify the distribution of PHA-L–labeled corticostriatal inputs to either the matrix or patch striatal compartments. The cortical areas injected were the infralimbic,

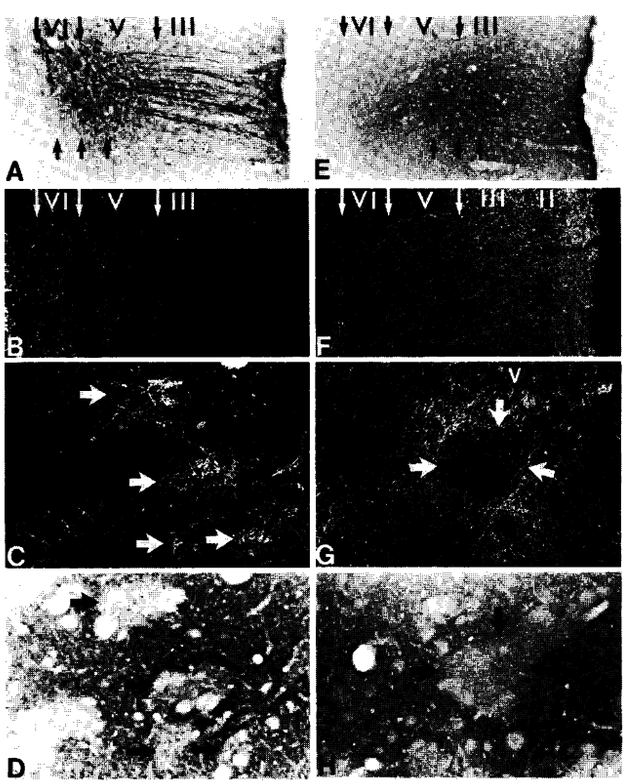

Fig. 1. Photomicrographs of PHA-L labeling after injections into the prelimbic cortex in two animals. In the first animal (A to D), PHA-L–injected neurons are located in layer VI and deep layer V (**A**). Axonal labeling is observed in the deep layers of the homotypic contralateral cortex (**B**) and in the striatal patches (arrows in **C**), which are marked by low levels of calbindin immunoreactivity in the adjacent section (arrows in **D**). In the second animal (E to H), PHA-L–injected neurons are located in upper layer V and in layers II and III (**E**). Axonal labeling is observed in the superficial layers of the contralateral homotypic cortex (**F**) and in the striatal matrix (**G**), which is marked by calbindin immunoreactivity in the adjacent section (**H**).

Laboratory of Cell Biology, National Institute of Mental Health, Building 36, Room 2D-10, Bethesda, MD 20892.